doi:10.1246/cl.2010.90

Published on the web December 26, 2009

Electrochemical Formation of Mg–Li–Yb Alloys at Solid Magnesium Electrode from LiCl–KCl–$YbCl_3$ Melts at Low Temperature

Ke Ye, Ye Chen, Milin Zhang,* Wei Han, Yongde Yan, and Shuquan Wei
Key Laboratory of Superlight Materials and Surface Technology, Ministry of Education, Harbin Engineering University, Harbin 150001, P. R. China

(Received October 27, 2009; CL-090954; E-mail: zhangmilin@hrbeu.edu.cn)

This work presents a novel study on electrochemical preparation of Mg–Li–Yb alloys at a magnesium electrode in LiCl–KCl–$YbCl_3$ melts at 743 K. Cyclic voltammograms showed that the reduction of ytterbium(III) ions is a stepwise reaction. The codeposition of Yb and Li takes place at magnesium electrode when the current intensity exceeds 60 mA in LiCl–KCl melts containing 2 wt % $YbCl_3$. α, $\alpha+\beta$, and β phases. Mg–Li–Yb alloys with different lithium contents were obtained by potentiostatic electrolysis at a magnesium electrode from LiCl–KCl melts with different concentrations $YbCl_3$.

Mg–Li alloys are known for their light weight and specific stiffness which are very attractive to the automotive, aerospace, and weapon industries.[1,2] However, poor thermal stability of Mg–Li binary alloys limits their wide applications. The addition of rare earth (RE) metals can enhance corrosion resistance as well as mechanical properties.[3]

Pure Mg, Li, and rare earth elements were directly casted for preparing Mg–Li–RE alloys in the traditional method, which has disadvantages such as inhomogeneous alloy composition and complicated production processes. To overcome these problems, electrochemical methods for the preparation of magnesium-based alloys are drawing increased attention. Our group[4,5] has successfully prepared Mg–Li alloys by electrolysis from LiCl–KCl melts on a magnesium cathode. The electrochemical formation and phase control of Mg–Li alloys at 693–783 K were investigated.

The codeposition of Mg–Li–Yb ternary alloys has not been investigated even though electrochemical codeposition has been widely used to prepare other alloys. Iida et al.[6–8] investigated the electrochemical codeposition of Sm–Co alloys from LiCl–KCl–$SmCl_3$–$CoCl_2$ melts and studied electrochemical formation of Yb–Ni and Sm–Ni alloy films by Li codeposition from chloride melts. Tsuda et al.[9–11] produced a series of Al-based alloys by codeposition from the molten salts of aluminum chloride–1-ethyl-3-methylimidazolium chloride. In this work, electrochemical behavior of Mg–Li–Yb alloys via codeposition at magnesium electrode from LiCl–KCl–$YbCl_3$ melts at 743 K was investigated by employing a series of electrochemical techniques.

A LiCl–KCl mixture (50:50 wt %, analytical grade) was contained in an alumina crucible placed in a quartz cell inside an electric furnace. The temperature of melts was measured with a nickel–chromium thermocouple sheathed by an alumina tube. The mixture was carefully purified. All experiments were performed under an argon atmosphere. The electrochemical techniques were performed using an Im6eX electrochemical workstation (Zahner Co., Ltd.). Ag/AgCl was used as reference electrode, which was constituted by a silver wire ($d = 1$ mm) dipped into a Pyrex tube containing a solution of AgCl (1 wt %) in LiCl–KCl melts. The working electrodes consisted of molybdenum ($d = 0.9$ mm) and magnesium rod ($d = 4$ mm). A spectral pure graphite rod ($d = 8$ mm) served as the counter electrode. The active electrode surface was determined after each experiment by measuring the immersion depth of the electrode. The deposits prepared by potentiostatic electrolysis were analyzed by XRD (X' Pert Pro; Philips Co., Ltd.) using Cu Kα radiation at 40 kV and 40 mA. The samples were dissolved and diluted in aqua regia, then the composition was determined by inductively coupled plasma atomic emission spectrometry (ICP-AES, Thermo Elemental).

Figure 1a shows typical cyclic voltammograms (CVs) obtained at a Mo electrode (curve 1) and a Mg electrode (curves 2 and 3) before and after the addition of 2 wt % $YbCl_3$ in LiCl–KCl melts at 743 K. The dotted curve 1 represents the voltammogram before the addition of $YbCl_3$ at a Mo electrode. A sharp increase in cathodic current from approximately −2.33 V (vs. Ag/AgCl) is observed. The cathodic signal B can be ascribed to the deposition of Li, since no alloys or intermetallic compounds exist for a Mo–Li binary system at 743 K.[12] In the reverse scan, an anodic peak B′ corresponding to the dissolution of Li is observed. The dash curve 2 shows the voltammogram before the addition of $YbCl_3$ at a Mg electrode. A cathodic current is seen from about −2.12 V. Since this potential value is more positive than that of Li metal deposition, the cathodic current is thought to be caused by the formation of Mg–Li alloys. The potential shift is due to a lowering of activity of the deposited metal (Li) in the Mg phase. Afterward, a group of signals B/B′ originating from the deposition/dissolution of Li appear. An anodic current corresponding to Li dissolution from the Mg–Li alloys is observed. No additional reoxidation peaks are observed in the anodic region. After adding 2 wt % $YbCl_3$, peak A_1 associated with reduction of Yb(III) to Yb(II)

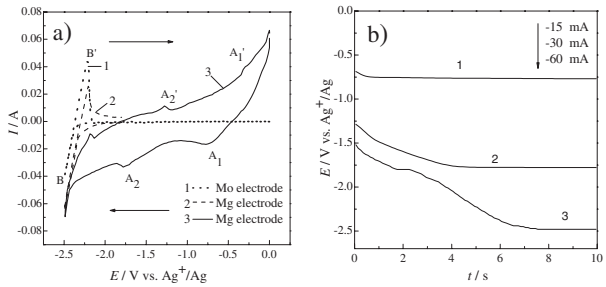

Figure 1. (a) Cyclic voltammograms of LiCl–KCl melts before and after the addition of 2 wt % $YbCl_3$ at a Mo electrode ($S = 0.104$ cm^2; curve 1) and a Mg electrode ($S = 0.457$ cm^2; curves 2 and 3) at 743 K. Scan rate: 0.1 V s^{-1}; (b) Chronopotentiograms obtained in LiCl–KCl–$YbCl_3$ (2 wt %) melts with various current intensities at a Mg electrode ($S = 0.457$ cm^2) at 743 K.

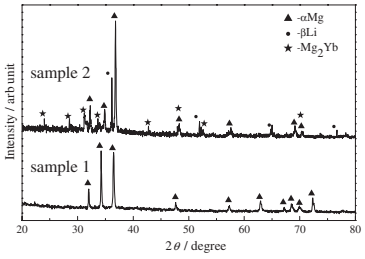

Figure 2. XRD patterns of sample 1 and sample 2 (followed by a postthermal treatment at 973 K) at −1.80 and −2.40 V (vs. Ag^+/Ag) obtained at Mg electrodes ($S = 0.457\,cm^2$) in the LiCl–KCl–$YbCl_3$ (2 wt %) melts by potentiostatic electrolysis for 3 h at 743 K, respectively.

ions was first detected at about −0.77 V in solid curve 3. Afterward, a cathodic current was observed. According to the phase diagram of the Mg–Yb system,[12] the cathodic current A_2 probably corresponds to the formation of Mg–Yb alloys. Similar phenomena were seen in the literature.[7,13,14] Finally, the cathodic signal B observed in the cathodic limit is ascribed to the formation of Mg–Li–Yb alloys. In the anodic direction, peaks B′ and A_2′ correspond to the dissolution of Li(0) and Yb(0) from the Mg–Li–Yb alloys, respectively. Afterward, anodic peak A_1′ can be ascribed to the oxidation of Yb(II) to Yb(III) ions.[7,13,14]

Chronopotentiometric experiments were carried out to further study the formation of Mg–Li–Yb alloys, as shown in Figure 1b. The first potential plateau 1 (−0.77 V) should be associated with the reduction of Yb(III) to Yb(II) ions, and the second potential plateau 2 (−1.77 V) could be ascribed to the reduction of Yb(II) ions to Yb(0). Up to current intensity of 60 mA, the curves started to exhibit two potential plateaus (plateaus 2 and 3) ascribed to the reduction of Yb(II) and Li(I) ions into metals, respectively. When the current intensity exceeds 60 mA, the codeposition of Yb and Li takes place at magnesium electrode to form Mg–Li–Yb alloys. It is obvious that the potential ranges of deposition of Yb and Li are the same as those observed in the CVs.

Based on the results obtained by cyclic voltammetry and chronopotentiometry, potentiostatic electrolysis experiments were conducted in the LiCl–KCl–$YbCl_3$ (2 wt %) melts for 3 h using Mg electrodes as working electrode at −1.80 V (sample 1) and −2.40 V (sample 2). Figure 2 shows the XRD patterns of samples 1 and 2. The reference XRD data for α, β, and Mg_2Yb phases (JCPDS No. 35-0821, No. 15-0401, and No. 50-1032) were used. The diffraction peaks for sample 1 could be assigned to α-Mg phase, indicating the Yb and Li contents in Mg–Li–Yb alloys were relatively low. However, typical $\alpha + \beta$ phase Mg–Li–Yb alloys were formed when the applied potential is at −2.40 V. The observed peaks for sample 2 are identified as $(\alpha + \beta) + Mg_2Yb$ phases. The ICP analyses of all samples obtained by potentiostatic electrolysis are listed in Table 1. Under potentiostatic electrolysis, the more negative the applied potential in the LiCl–KCl melts with equivalent $YbCl_3$ concentration, the higher the Li and Yb contents of Mg–Li–Yb alloys.

As the applied potential is at −1.80 V, sample 1 prepared by potentiostatic electrolysis are basically pure Mg. However, when the applied potential negatively shifts to −2.40 V, an $\alpha + \beta$ phase Mg–Li–Yb alloy (Li 8.21 wt %) was obtained. The ICP results are in good agreement with the phase structures of the XRD patterns. It is obvious that the Li contents of the Mg–Li–Yb alloys increase (from α to β phase) with negative shifts in the applied potential. In addition, the Yb contents of Mg–Li–Yb alloys increase with increasing $YbCl_3$ concentrations in the LiCl–KCl melts.

Table 1. The ICP analyses of all samples (followed by a post-thermal treatment at 973 K) obtained by potentiostatic electrolysis at Mg electrodes ($S = 0.457\,cm^2$) from the LiCl–KCl melts containing different $YbCl_3$ concentrations for 3 h at 743 K

Samples	$YbCl_3$ concentration /wt %	Electrolytic potential /V	Li content /wt %	Yb content /wt %	Mg content /wt %
1	2	−1.80	0.53	0.16	Bal.
2	2	−2.40	8.21	1.86	Bal.
3	2	−2.30	2.37	0.65	Bal.
4	2	−2.50	19.69	2.47	Bal.
5	1	−2.40	8.65	0.93	Bal.
6	3	−2.40	9.03	2.09	Bal.

In summary, α, $\alpha + \beta$, and β phases Mg–Li–Yb alloys with different Li contents (0.53–19.69 wt %) were prepared by potentiostatic electrolysis at Mg electrode, and the Li and Yb contents of Mg–Li–Yb alloys could be controlled by $YbCl_3$ concentration and applied potential. Mg–Li–Yb alloys prepared directly from LiCl–KCl–$YbCl_3$ melts at solid magnesium electrode at low temperature will be revolutionary in the Mg–Li–RE alloys industry.

The work was financially supported by the 863 Project of the Ministry of Science and Technology of China (No. 2006AA03Z510), the National Natural Science Foundation of China (No. 50871033), the Scientific Technology Project of Heilongjiang Province (No. GC06A212), and the Scientific Technology Bureau of Harbin (No. 2006PFXXG006).

References

1 Z. Drozd, Z. Trojanová, S. Kúdela, *J. Alloys Compd.* **2004**, *378*, 192.
2 A. Sanschagrin, R. Tremblay, R. Angers, D. Dubé, *Mater. Sci. Eng., A* **1996**, *220*, 69.
3 M. L. Zhang, Y. D. Yan, W. Han, Y. Xue, X. Y. Jing, X. L. Liu, S. S. Wang, X. M. Zhang, *Electrochemistry* **2009**, *77*, 699.
4 M. L. Zhang, Y. D. Yan, Z. Y. Hou, L. A. Fan, Z. Chen, D. X. Tang, *J. Alloys Compd.* **2007**, *440*, 362.
5 Y. D. Yan, M. L. Zhang, W. Han, D. X. Cao, Y. Yuan, Y. Xue, Z. Chen, *Electrochim. Acta* **2008**, *53*, 3323.
6 T. Iida, T. Nohira, Y. Ito, *Electrochim. Acta* **2003**, *48*, 2517.
7 T. Iida, T. Nohira, Y. Ito, *Electrochim. Acta* **2003**, *48*, 1531.
8 T. Iida, T. Nohira, Y. Ito, *Electrochim. Acta* **2001**, *46*, 2537.
9 T. Tsuda, C. L. Hussey, G. R. Stafford, J. E. Bonevich, *J. Electrochem. Soc.* **2003**, *150*, C234.
10 T. Tsuda, C. L. Hussey, G. R. Stafford, *J. Electrochem. Soc.* **2004**, *151*, C379.
11 T. Tsuda, C. L. Hussey, G. R. Stafford, O. Kongstein, *J. Electrochem. Soc.* **2004**, *151*, C447.
12 T. B. Massalski, J. L. Murray, L. H. Benett, H. Baker, *Binary Alloy Phase Diagrams*, American Society for Metals, Cleveland, OH, **1990**.
13 Q. Yang, G. Liu, Y. Tong, Y. Ao, Y. Su, *Rare Met.* **1996**, *15*, 59.
14 V. Smolenski, A. Novoselova, A. Osipenko, C. Caravaca, G. Córdoba, *Electrochim. Acta* **2008**, *54*, 382.

